Supplement of Biogeosciences, 21, 3239–3250, 2024
https://doi.org/10.5194/bg-21-3239-2024-supplement

Biogeosciences Open Access EGU

Supplement of

Variable contribution of wastewater treatment plant effluents to downstream nitrous oxide concentrations and emissions

Weiyi Tang et al.

Correspondence to: Weiyi Tang (weiyit@princeton.edu)

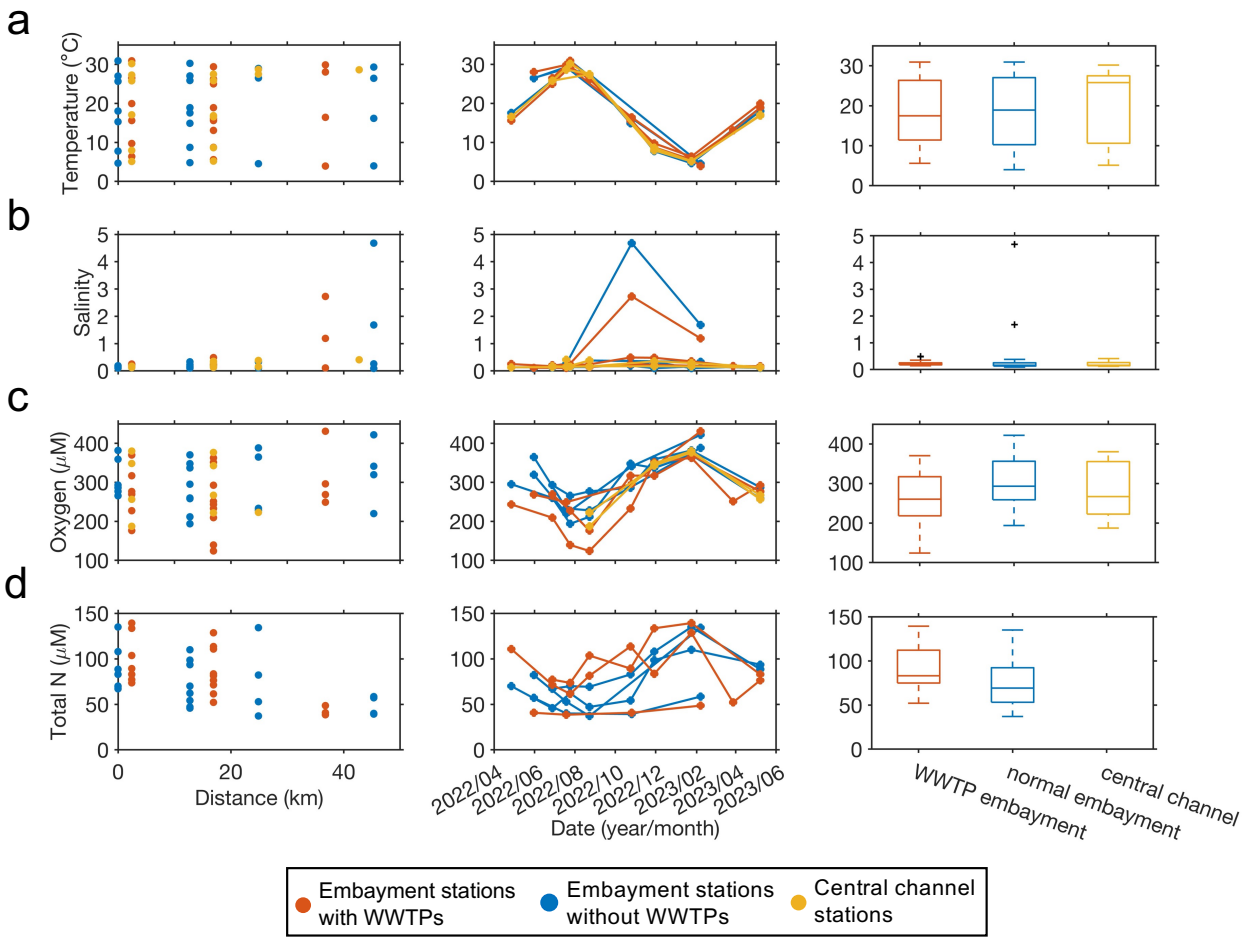

Fig. S1. Spatial and temporal variations of temperature (a), salinity (b), oxygen (c) and total nitrogen concentration (d). The distance shows from upstream to downstream stations in the Potomac River. Embayment stations associated with wastewater treatment plants (WWTPs, red circles and lines) and without WWTPs (blue circles and lines), and central channel stations (yellow circles and lines). Total N concentration was not measured at central channel stations. For the boxplots, the red line in each box is the median. The bottom and top of each box are the 25th and 75th percentiles of the observations, respectively. The error bars represent 1.5 times the interquartile range away from the bottom or top of the box, with red + signs showing outliers beyond that range.

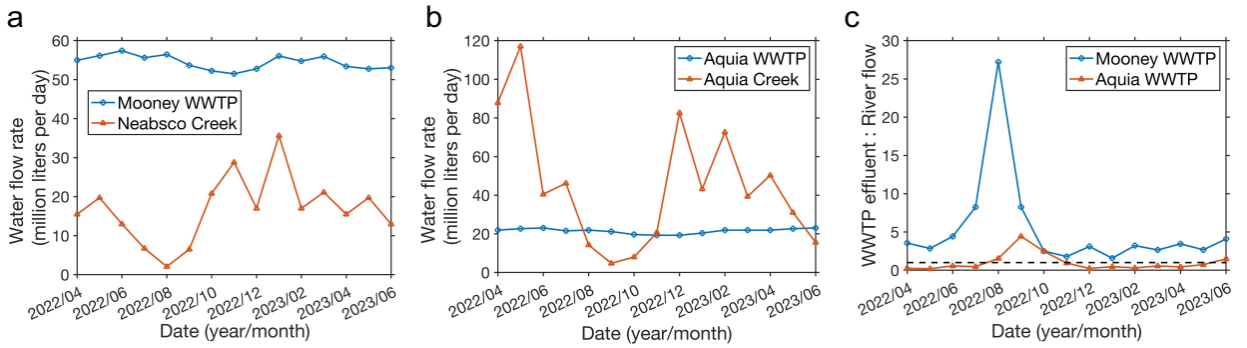

Fig. S2. Comparison between wastewater treatment plants effluents and riverine discharge. (a) Mooney WWTP vs Neabsco Creek. (b) Aquia WWTP vs Aquia Creek. (c) the ratio of wastewater treatment plants effluents to riverine discharge. The horizontal dashed line denotes a ratio of 1. Riverine discharges at monitoring stations upstream of the Mooney WWTP (monitoring station of Neabsco Creek at Dale City, Virginia) and Aquia WWTP (monitoring station of Aquia Creek near Garrisonville, Virginia) were obtained from United States Geological Survey (USGS). Climatological riverine discharge was used for Neabsco Creek because data were not available for years 2022 and 2023.

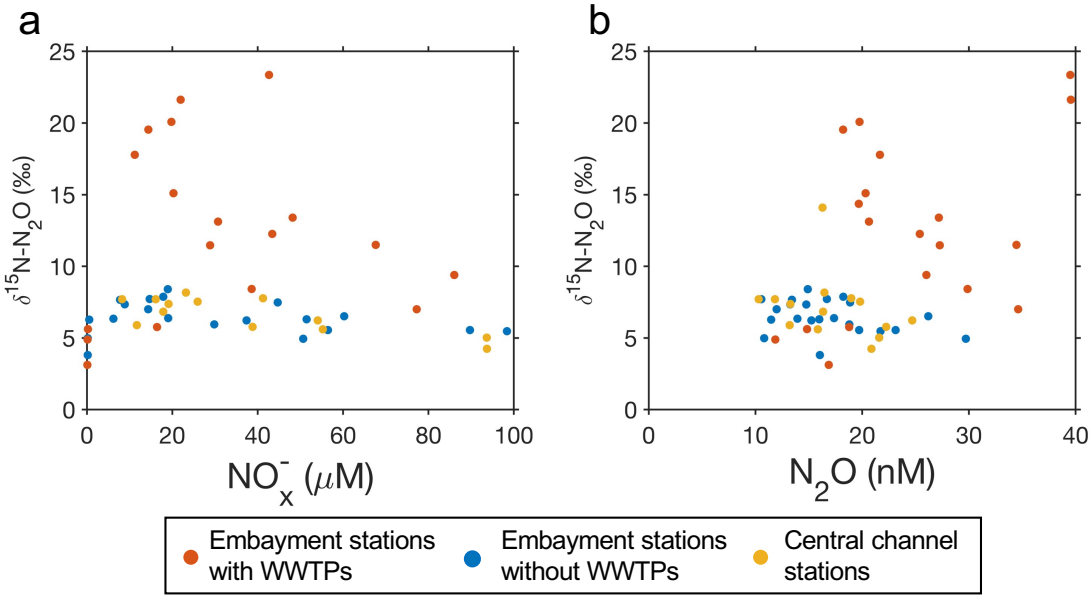

Fig. S3. The change in $\delta^{15}N$ of N_2O in relation to the changes in NO_x^- concentrations (a) and N_2O concentrations (b).

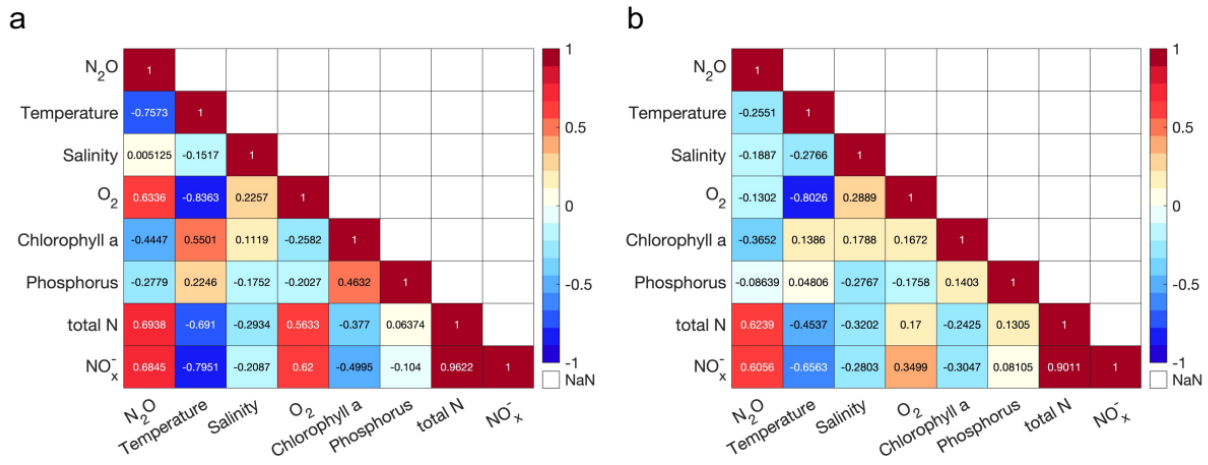

Fig. S4. Correlation coefficients among different environmental factors and N_2O concentration for stations without (a) or with (b) the influence of WWTPs.

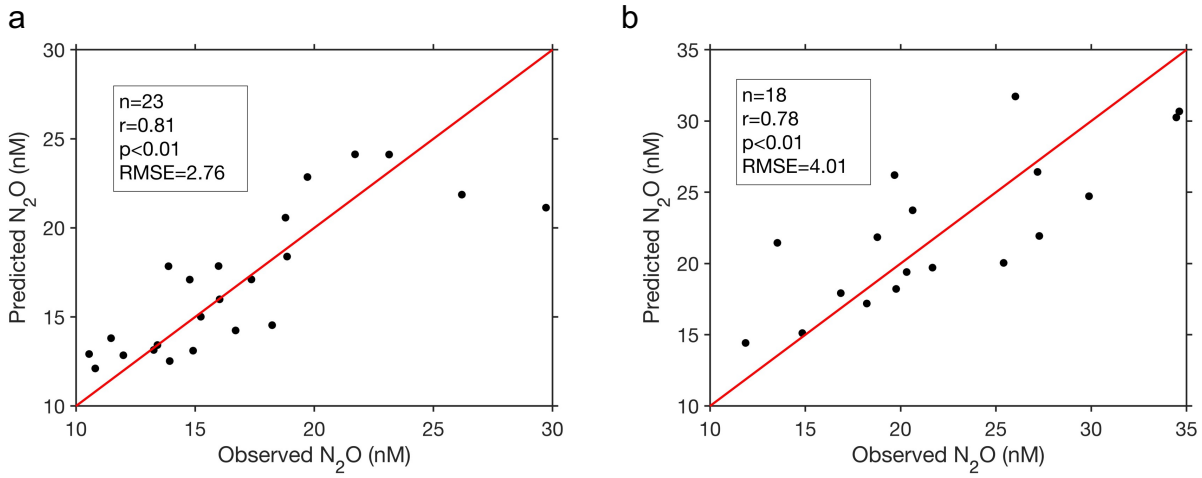

Fig. S5. Predicted versus observed N_2O concentration based on a multiple linear regression model for stations without (a) or with (b) the influence of WWTPs. The number of data points (n), correlation coefficient (r), p value and root mean square error (RMSE) are presented in the legend.

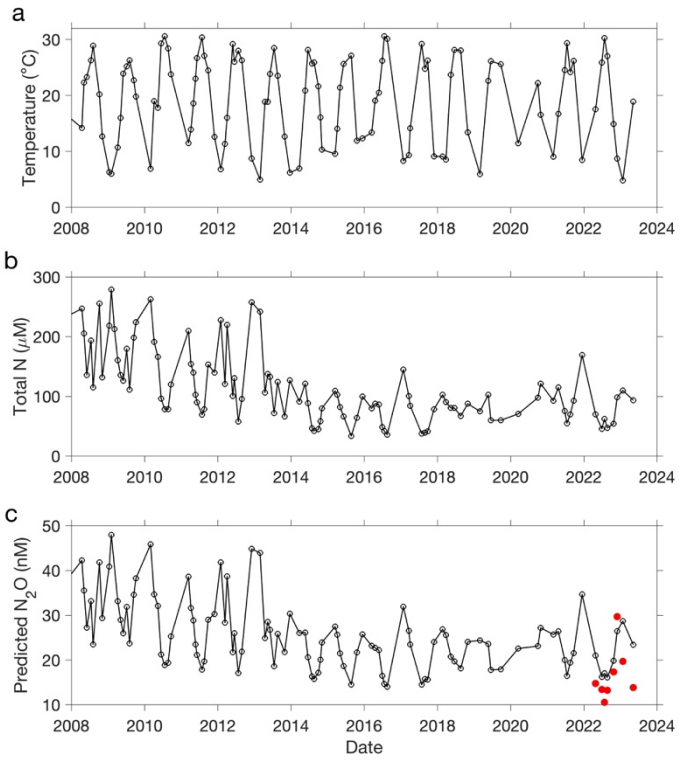

Fig. S6. Historical measurements of temperature (a) and N concentration (b) at the Pohick Bay sampling station with the influence of Noman Cole WWTP. N_2O concentration (c) is predicted based on a multiple linear regression model developed for stations with the influence from WWTPs. The red points are the observed N_2O concentration.

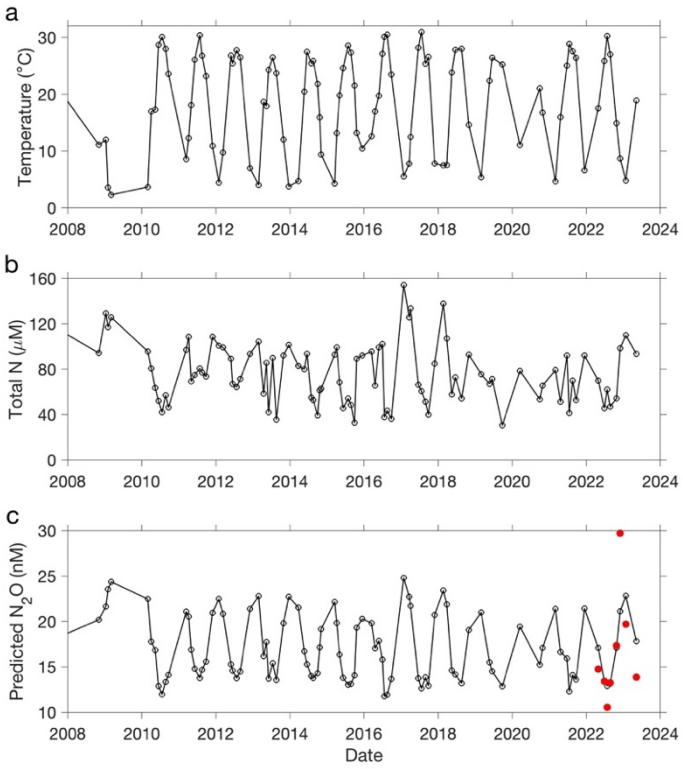

Fig. S7. Historical measurements of temperature (a) and N concentration (b) at the Occoquan Bay sampling station without the influence of WWTPs. N_2O concentration (c) is predicted based on a multiple linear regression model developed for stations without the influence from WWTPs. The red points are the observed N_2O concentration.

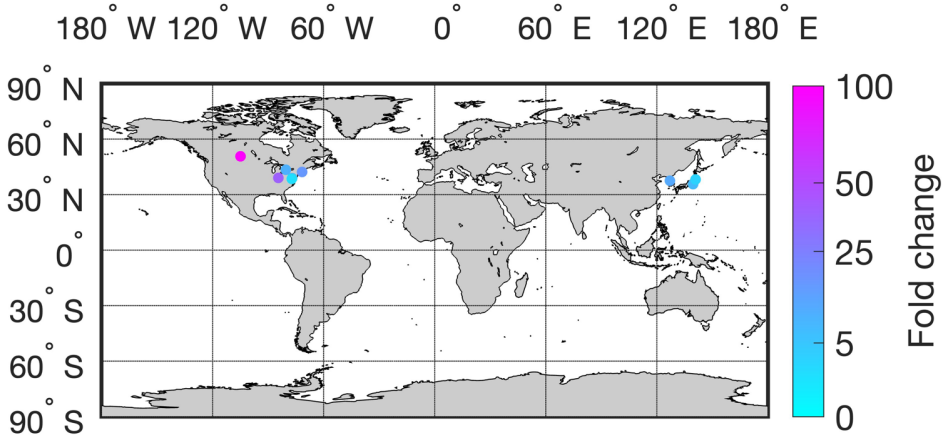

Fig. S8. N_2O observations associated with WWTPs globally, color-coded by the fold change in N_2O concentration, saturation or flux comparing downstream and upstream of WWTPs (see Table 1 for details).